

Temperature Variation Analysis of the STIM300 Inertial Measurement Unit

Ivan Rodrigues Bertaska, Ph.D.

EV41 Control Systems Design and Analysis, Marshall Space Flight Center, Huntsville, AL 35812

I. Introduction

A key navigation instrument found on most autonomous and semi-autonomous platforms is the inertial measurement unit (IMU). This type of sensor is a combination of microelectromechanical systems (MEMS) that provide inertial information to the navigation system. Typical MEMS hardware include a gyroscope and an accelerometer (for rates and accelerations, respectively) within a single platform. The Near Earth Asteroid (NEA) Scout mission, slated to launch in October of 2018 (Author's note: NEA Scout ultimately launch on November 16, 2022), carries an on-board IMU from Sensoror. This particular model has yet to see spaceflight, and questions about its on-orbit reliability remain. Dynamic tests were produced in the summer of 2016 by a visiting faculty member from Arkansas Tech University, Daniel Bullock. During these experiments, concerns about the noise characteristics of the sensor were raised, specifically relating to how temperature fluctuations affected the unit. It was found that the IMU took an extended period of time before reaching an internal steady state temperature. These tests often displayed large temperature variations, making the calculation of noise characteristics, such as bias drift, difficult to attribute entirely to noise. Static and dynamic tests were re-performed under more stringent constraints on temperature. Tests reported herein conclude that the IMU is adequately capable of providing inertial information for the NEA Scout mission.

II. Experimental Setup

A. STIM300 Overview

Table 1 displays some basic information on the STIM300 unit. There are several major differences between the static tests performed in this paper and those performed by Dr. Dan Bullock in his report:

- The internal cascaded integrator-comb (CIC) filter of the IMU was set to the lowest possible bandwidth to reject the absolute maximum amount of noise without post-processing ($f_c = 16\text{Hz}$).
- Static tests were performed over significantly longer periods of time, allowing for the calculation of the root Allan variance plots. From these plots, key noise characteristics could be found, such as angular random walk (ARW) and in-run bias instability (IRBS).
- Temperature was controlled in a thermally and structurally isolated chamber to within 0.5°C of a set point.

NEA Scout is using the STIM300 exclusively for rate information. Out of brevity, only gyroscope data (i.e., rate information) is included in this report. Further information from the accelerometer can be found the Dr. Dan Bullock's Final Report.

B. STIM300 Test Setup and Procedure

A mount was designed and 3D printed, capable of housing the STIM300, a 10000mAh Li-ion battery, and a small single board computer to collect data from the IMU within the thermal chamber. The chosen SBC was the Raspberry

Table 1 – STIM300 Manufacturer Characteristics

Sensors	Gyroscope, accelerometer, inclinometer
Temperature Range	-40°C to 85°C
Interface	RS-422
Baud Rate	$< 1,000,000$ bps
Voltage	5V
Absolute Maximum Rate	$400^\circ/\text{s}$
Absolute Maximum Acceleration	10g

Pi B, due to its low cost and prevalence in the hobby-grade community. Tests were performed in a thermally isolated chamber in 4487/A112. Aside from being temperature-controlled, the testing room was structurally isolated from the remainder of the building, and its foundation was sunk further into the bedrock than surrounding structures. This prevented parasitic vibrations (e.g., passing trucks) from interfering with test results.

Due to the long settling time before temperature reached an equilibrium, tests were run for a minimum of three hours, and limited to five hours due to the battery life. Tests were performed under a wide range of temperatures from -20°C to 55°C. A picture of the thermal chamber is found in Figure 1. Data on the rotary table can be found in Table 2.

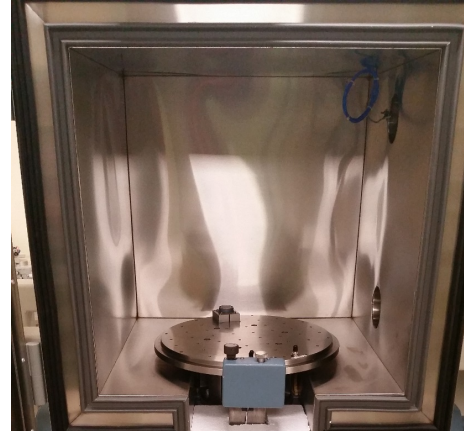


Figure 1 –Temperature-controlled thermal chamber with rotary table.

III. Results

A. Static Experimental Tests

Stationary tests were performed in the chamber to obtain key noise characteristics of the gyroscope. These were found using a plot known as the root Allan variance, which is capable of providing frequency-dependent noise characteristics, (e.g., white noise, pink noise, and red noise). Root Allan variance plots were generated from data sets at each target temperature. It was then straight forward to locate the ARW and IRBS for each experiment. Internal

Table 2 – 2-Axis Rate Table Model 352 with Thermal Chamber

Maximum size	20"x20"x20"
Maximum rate	1000°/sec
Roll axis rate accuracy	±2%
Pitch axis movement	0° (Thermal Chamber)
Pointing accuracy	±1 arcsec
Temperature range	-20°C to 70°C
Temperature accuracy	±1°F

Table 3 – Static Experiment Results

	Axis	Bias (°/hr)	Bias Drift (°/hr)	Standard Deviation (°/hr)	ARW (°/√hr)	IRBS °/hr
Factory Calibration Report	X	8.2	4	131.04	0.1378	0.6463
	Y	-36.9	3	136.44	0.1461	0.4907
	Z	8.6	4	153.72	0.161	0.8486
T = -20C	X	-262.9584	-0.365796	39.8844	0.12137	0.43882
	Y	-176.0868	0.3366324	39.186	0.1171	0.34964
	Z	-100.044	2.235672	45.2988	0.13565	0.51464
T = 0C	X	-229.5792	-2.820492	43.5492	0.12904	0.59642
	Y	-186.6528	0.884772	45.8064	0.13352	0.26442
	Z	-109.6236	0.590112	52.884	0.1548	0.74585
T = 20C	X	-170.5212	0.392688	47.8368	0.14641	0.29635
	Y	-179.694	1.020636	51.9156	0.15802	0.46621
	Z	-116.622	-1.488996	57.474	0.17651	0.62836
T = 40C	X	-151.2756	2.485152	55.1592	0.14896	0.64165
	Y	-178.6716	-1.092456	55.8648	0.15051	0.23346
	Z	-104.2272	1.487808	64.6308	0.17367	0.50463
T = 55C	X	-155.7648	-2.713572	58.248	0.16778	0.84631
	Y	-198.0828	-2.217996	62.0856	0.17711	0.29449
	Z	-114.9336	-2.099592	71.37	0.20664	0.53844

temperature data was collected using the nine thermal sensors located within the STIM300. Data sets only incorporated gyroscope readings when the thermal sensors registered a steady-state temperature. Temperature fluctuations were kept at a minimum to produce gyroscope outputs with the highest achievable fidelity, unaffected by possible temperature gradients across the sensor.

Table 3 displays the results for each temperature, as well as the values derived from the factory calibration report. It should be noted that the calibration report used a different configuration of the STIM300 with a higher sampling rate ($f_s = 250\text{Hz}$) and higher CIC-filter cutoff frequency ($f_c = 33\text{Hz}$). The experimental setup had the STIM300 producing outputs at the lowest sampling rate, $f_s = 125\text{Hz}$, with the lowest cutoff frequency, $f_c = 16\text{Hz}$. This is expected to be configuration of the sensor in flight.

Temperature-correlated statistical parameters could then be plotted to examine how temperature fluctuations affected the gyroscope output. One such plot is found Figure 2. Upon closer inspection, it can be concluded that the steady-state bias displayed little variation across temperatures, with the possible exception of the X-axis. Bias drift also exhibited little difference across the tested temperature range, with deviations occurring in both the negative and positive domain. This implies that the bias drift is not linked to temperature, but rather, is a product of the noise characteristics itself. In this case, bias instability is related to pink noise, with a power spectral density (PSD) proportional to the inverse of frequency ($PSD \propto 1/f$). Unsurprisingly, the standard deviation exhibited a positive correlation to temperature increases. Thus, the power of the white noise in the sensor is diminished at lower temperatures, increasing as the ambient temperature rises.

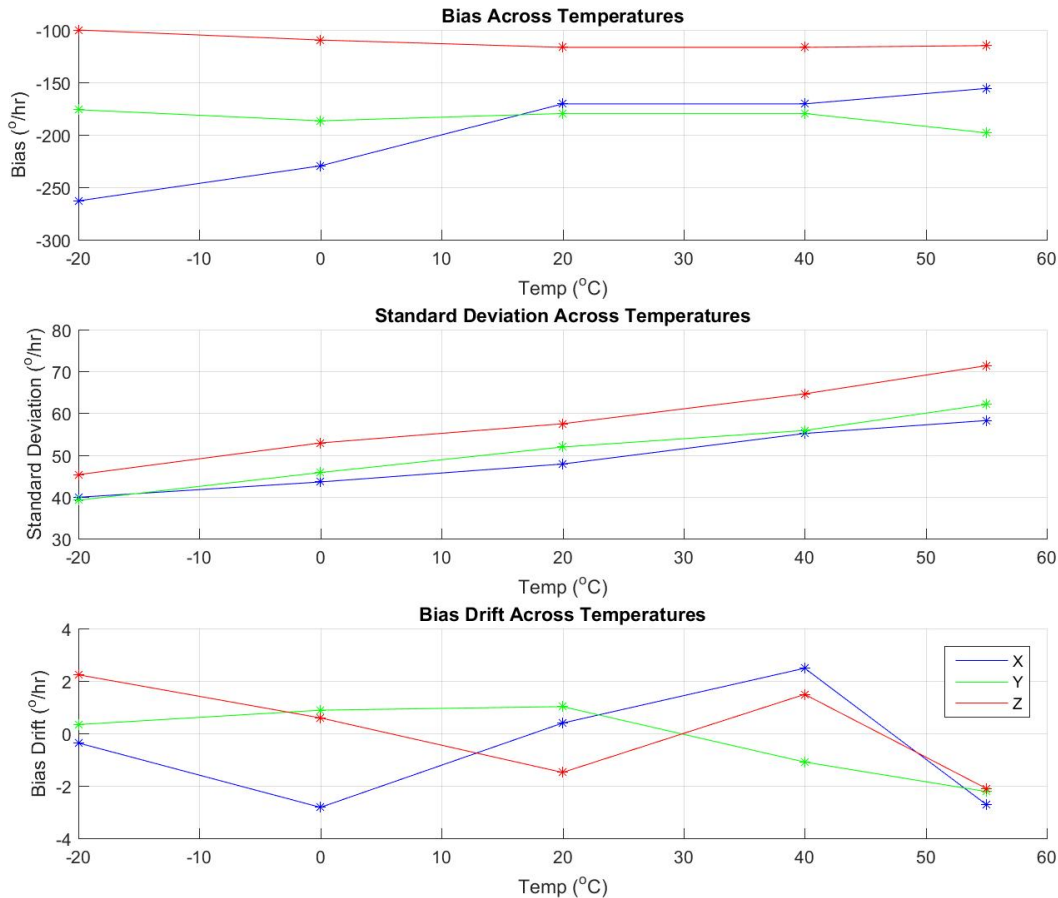


Figure 2 – Bias, standard deviation, and bias drift across the tested temperatures.

An example of the root Allan variance (i.e., Allan deviation) is found in Figure 3. The root Allan variance provides valuable insight into the effects of noise at generalized portions of the frequency spectrum. The straight downward trend of the graph implies that white noise is dominant across those cluster times and is the largest source of noise in the output of the gyroscope. Interestingly, the small peak at the $[10^{-2}, 10^{-1}]$ decade is a response of the CIC filter buffer, correlating outputs of the gyroscope with previous outputs. IRBS is defined at the minimum of the root Allan variance chart and provides the best-case scenario for a minimal drift in bias.

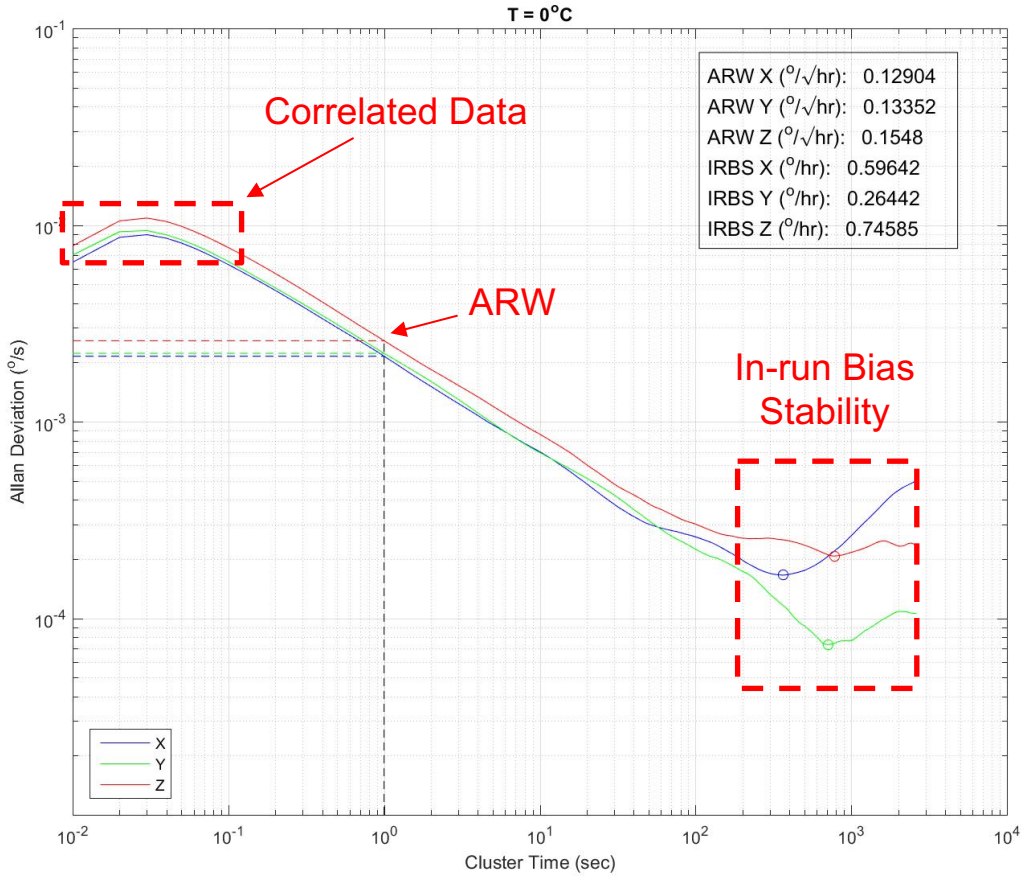


Figure 3 – Root Allan variance for the static experiment at T=0°C.

B. Dynamic Experiment Tests

A simple dynamic test was performed at the RSS of the highest expected rates across each of NEA Scout’s axes. The rate table temperature was set to near room temperature at T=26°C, and a desired rate was input as 17.32°/s. The rotary table continued to spin for three hours such that a stable temperature was guaranteed within the sensor. Plots of the results can be found below. Since the expected rates of NEA Scout’s mission are comparatively small, the gyroscope ought to function solely in its linear region of operation. Figure 4 displays the unfiltered results.

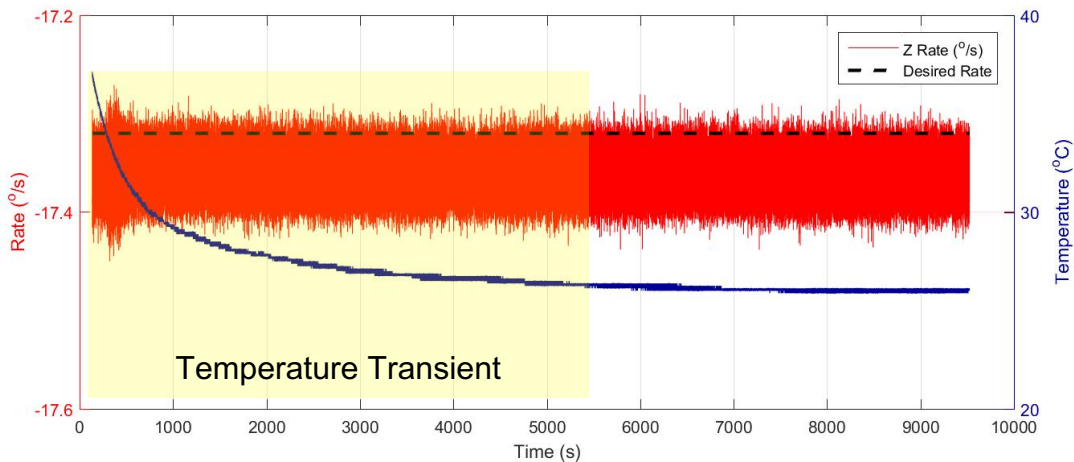


Figure 4 – Rotating experiment with RSS of maximum rotation rates across all three axis at T=20°C.

Table 4 displays a comparison between the static and rotating experiments at the setpoint temperature of $T=0^{\circ}\text{C}$. The gyroscope was able to correctly identify the desired rate with a steady state bias comparable to that of the static case. The major difference between the two experiments was in the X-axis and Y-axis biases. This discrepancy implies that there is a misalignment of the MEMS gyroscope, which the factory calibration report explicitly gives. This misalignment is taken into account in the gyroscope model within NEA Scout's simulation environment. Mounting of the unit also contributed to this error.

Table 4 – Comparison of rotating and static experiments

	Axes	Mean (°/s)	Bias (°/s)	Standard Deviation (°/s)	Average Temperature (°C)
Rotating	X	-0.070256	-0.070256	0.013715	26.1021
	Y	0.005658	0.005658	0.014749	26.1207
	Z	-17.36078	-0.04019	0.016468	26.1172
Static	X	-0.047367	-0.047367	0.013288	25.0330
	Y	-0.049915	-0.049915	0.014421	25.0590
	Z	-0.032395	-0.032395	0.015965	25.0417

IV. Conclusions

A few major conclusions drawn from the temperature controlled experiments:

- The internal temperature of the IMU took an extended period of time before reaching a steady state value (often over 2 hours for extreme temperatures).
- Experimental data closely matched, or exceeded in reliability, calibration report parameters, with the exception of the steady-state angular rate bias.
- White noise dominated the noise spectrum of the sensor, but bias stability ought to still be considered when modeling the sensor.
- From simulations, the Kalman filter was adequately able to determine the steady-state bias of the sensor. When propagating attitude based solely on IMU rates, the spacecraft was able to maintain attitude knowledge to within 0.36° of the true attitude.
- Buffering the IMU rate data and then subsequently averaging it would significantly reduce the effect of white noise on the system.